

Non-thermal transient sources from rotating black holes

Maurice H.P.M. van Putten

Le Studium IAS, 3D Avenue Recherche Scientifique, 45071 Orléans Cedex 2, France

Alok C. Gupta

Aryabhata Research Institute of Observational Sciences (ARIES), Manora Peak, Nainital - 263129, India

ABSTRACT

Rotating black holes can power the most extreme non-thermal transient sources. They have a long-duration viscous time-scale of spin-down and produce non-thermal emissions along their spin-axis, powered by a relativistic capillary effect. We report on the discovery of exponential decay in BATSE light curves of long GRBs by matched filtering, consistent with a viscous time-scale, and identify UHECRs energies about the GZK threshold in linear acceleration of ion contaminants along the black hole spin-axis, consistent with black hole masses and lifetimes of FR II AGN. We explain the absence of UHECRs from BL Lac objects due to UHECR emissions preferably at appreciable angles away from the black hole spin-axis. Black hole spin may be key to unification of GRBs and their host environments, and to AGN and their host galaxies. Our model points to long duration bursts in radio from long GRBs without supernovae and gravitational-waves from all long GRBs.

1. Introduction

Recent developments in high-energy observations reveal a transient universe abundant in non-thermal emissions across an exceptional range in energies, from radio, as in a recent report on an extragalactic < 5 ms radio-burst (Lorimer et al. 2007), to gamma-rays in cosmological GRBs, and ultra-high energy cosmic rays (UHECRs) at energies of 10^{19} eV (Abraham et al. 2007).

Attributing non-thermal emissions and outflows to black holes is attractive, as it provides an ideal site for converting gravitational potential energy into various emission channels, by dissipation in an accretion disk or interactions with the spin of the black hole. Non-Newtonian behavior of the radiation processes poses novel observational challenges which

may invite novel methods of data-analysis and novel probes of the “physics inside” by neutrino emissions or gravitational-waves (Aspera 2008).

Here, we focus on rotating black holes as a potentially common engines to the most energetic non-thermal transient sources. They are described by their mass and angular momentum (generally with a modest electric charge in a state of equilibrium). The outcome may depend on black hole spin and whether accretion disks are sufficiently magnetized to create magnetic outflows. The physical state of nuclei is therefore important to unification schemes of AGN and quasars (Antonucci 1993; Urry & Padovani 1995; Jackson & Wall 1999) in understanding radio-morphologies, continuum and line-emissions and, possibly, variability. The Fanaroff-Riley I and II radio-galaxies Fanaroff & Riley (1974) may serve as an example, possibly with distinctions in the presence or absence of a hidden quasar Antonicci (2008). The total luminosity alone, however, is sufficient to identify black hole spin (Livio et al. 1999).

The Pierre Auger Observatory provides the first angular correlation between UHECRs with nearby AGN in the catalogue of Véron-Cetty & Véron (2006). The AGN identified appear to trace nearby spiral galaxies, based on the complete HI Parkes All Sky Survey (HIPASS) Ghisellini et al. (2008). It might suggest that stellar mass transients or dormant AGN (Levinson 2001) be the source of the observed UHECRs. However, this does not account for the paucity of UHECRs in the Virgo cluster (Zaw et al. 2008) or the apparent absence of UHECRs with blazars (Harari 2007). Classification of the associated AGN remains tentative, because the VCV catalogue is not complete and may not be an unbiased sample of the AGN Zoology. Based on the combined NASA/IPAC Extragalactic Database (NED), UHECRs appear to be associated with low-luminosity Seyfert galaxies and LINERs with relatively few radio galaxies (Moskalenko et al. 2008). There may be a minimum bolometric luminosity for UHECRs to ensue, consistent with the paucity of UHECRs from the Virgo cluster (Zaw et al. 2008). UHECRs associated with radio-galaxies (Nagar & Matulich 2008), may originate in large radio-lobes of FR II AGN (Fraschetti 2008; Frascetti & Melia 2008). This would require the radio-jet to be baryon-rich, to account for the observed proton and heavier elements in the UHECRs. It would produce largely isotropic emissions in UHECRs inconsistent with the paucity of UHECRs from blazars that are hiding FR IIs, and does not account for the apparent association with Seyfert galaxies and LINERs. Instead, UHERs may indeed be produced by some of the galactic nuclei. If confirmed, “UHECR-active” and “UHECR-inactive” nuclei promises a significant extension to AGN classification and unification schemes.

In this *Letter*, we consider two first-principle physical properties of rotating black holes: a long-duration viscous time-scale of spin-down and ultra-high energy emissions induced by

a relativistic capillary effect along the spin-axis (van Putten 2008b):

- Exponential decay in the long duration evolution of GRB light curves, identified by application of matched-filtering to the BATSE catalogue on the premise that the inner engine of long GRBs is long-lived (Piran & Sari 1998). The template used is generated by spin-down of a Kerr black hole interacting with high-density matter at critical magnetic stability (van Putten & Levinson 2003).
- Creation of UHECRs in a linear accelerator powered by a relativistic capillary effect in the funnel along the spin axis of the black hole surrounded by an ion torus – typical for AGN – with energies that are tightly correlated to the mass of the supermassive black hole and the lifetime of the AGN. The latter has recently been studied in some detail for the FR II radio-galaxies (O’Dea et al. 2008).

We discuss the application to unification schemes for all GRBs – long and short, with and without supernovae (the *Swift* event GRB 060614, Della Valle (2006)) – and UHECR-active AGN. We begin with an introduction to the relevant physical properties of Kerr black holes, and apply these to the active nuclei of transient sources. We describe specific observational tests to enable a comparison with observations, present and in the future.

2. Some physical properties of Kerr black holes and surrounding matter

Rotating black holes in astrophysical environments introduce at least two unique physical properties: a long-duration timescale of spin-down associated with a large reservoir in spin-energy, and linear-acceleration to ultra-high energies along their spin axis.

Rotating black holes (Kerr 1963) are described by their mass M , angular momentum J , specific angular momentum $a = J/M$, and spin-energy $E_s = \frac{1}{2}\Omega_H^2 I f_s^2$, where $\sin \lambda = a/M$ (van Putten 1999) with relativistic correction factor $0.7654 < f_s = \frac{\cos(\lambda/2)}{\cos(\lambda/4)} < 1$ for the angular velocity $\Omega_H = \frac{1}{2M} \tan(\lambda/2)$, and where $I = 4M^3$ denotes the moment of inertia in the limit of slow rotation (Thorne et al. 1986). Thus, E_s/M can reach 29% ($\lambda = \pm\pi/2$), larger than the spin energy per unit mass in neutron star by an order of magnitude. Kerr black holes evolve according to the first law of thermodynamics $dM = \Omega_H dJ + T_H dS$ for changes in spin energy, $dE_s = \Omega_H dJ$, and dissipation, $dQ = T_H dS_H$, with Bekenstein-Hawking entropy (Bekenstein 1973), $S_H = 4\pi M^2 \cos^2(\lambda/2)$. In the limit of viscous spin-down with no radiation, we note that S_H *doubles* in spin-down to zero from an initial state of maximal spin.

Frame-dragging creates *linear acceleration* by coupling of the Riemann tensor to the angular momentum J of charged particles along open magnetic flux-tubes about the spin-

axis of a black hole. In geometrical units, the product of the Riemann tensor (cm^{-2}) and angular momentum (cm^2) is of dimension 1, which represents a force (Papapetrou 1951). Integration along a semi-infinite line to infinity produces a potential energy. In Boyer-Lindquist coordinates we have, along the spin-axis of the black hole (van Putten 2000, 2005, 2008b),

$$\mathcal{E}(r) = \int_r^\infty \text{Riemann} \times J ds = \omega J. \quad (1)$$

The ensuing *relativistic capillary effect* extracts e^\pm -pairs from the environment of the black hole, where they are created by canonical pair-cascade processes (Blandford & Znajek 1977), out to larger distance along the spin-axis (van Putten 2000). A transition to a nearly force-free state (Blandford & Znajek 1977) terminates in an outgoing Alfvén front. Thus, the raw Faraday-induced horizon potential (1) is communicated to the outgoing Alfvén front. Since magnetic flux-surfaces *upstream* are stable against pair-cascade, they remain largely charge-free, and become clean site for linear acceleration of baryonic contaminants, ionized by exposure to ambient UV-radiation.

In its lowest energy state the horizon flux Φ_θ^e of a magnetic field with strength B through a polar cap of half-opening angle θ_H is, adapted from Wald (1974), $\pi B \frac{(r_H^2 + a^2)^2}{r_H^2 + a^2 \cos^2 \theta} \sin^2 \theta$, where $r_H = 2M \cos^2(\lambda/2)$ and $a = M \sin \lambda$. The full horizon flux ($\theta = \pi/2$) $\Phi_H^e = 4\pi B M^2$ is hereby the same for maximal rates and zero-spin, while through a polar cap ($\theta \ll \pi/2$), $\Phi_\theta^e \simeq 2\pi B M^2 \theta^2$ about maximal spin (and a factor two larger at zero spin). The Faraday induced potential energy on a flux tube with $A_\phi = B M^2 \theta^2$ at $r = r_H$ in (1), is

$$\mathcal{E}(\theta) = ec\partial_t \Phi = e\Omega_H A_\phi \simeq \frac{1}{2} e B M \theta^2 = 2.16 \times 10^{20} B_5 M_9 \theta^2 \text{ eV} \quad (2)$$

in the limit of maximal spin ($\Omega_H \simeq 1/2M$), where $\theta \leq \theta_H$. The lifetime of spin of a supermassive black hole is largely based on dissipation $T_H \dot{S}_H$ in the event horizon. The average is about $\frac{1}{3}$ -rd of the maximal dissipation rate, i.e.:

$$\langle \dot{Q} \rangle = \frac{c}{3} (\Omega_H A_\phi)^2 = \frac{c}{12} B^2 M^2 = 5.6 \times 10^{47} (B_5 M_9)^2 \text{ erg s}^{-1} \quad (3)$$

The lifetime of spin for a maximally spinning black hole hereby becomes $T \simeq 29\% \times 2 \times 10^{63} M_9 \text{ erg} \langle \dot{Q} \rangle^{-1}$, whereby $B_5 M_9^{1/2} T_7^{1/2} \simeq 1.04$, or

$$B_5 M_9 = 1.04 \sqrt{\frac{M_9}{T_7}} \quad (4)$$

with $T = T_7 10^7 \text{ yr}$ following O’Dea et al. (2008). With conservation of flux, $B \simeq 10^5 \text{ G}$ at the ISCO may be compared with $B \sim 10^{-2} \text{ G}$ fields on sub-parsec scales in Mrk 501

(O’Sullivan & Gabuzda 2008). Scaling to stellar mass black holes surrounded by high-density matter with superstrong magnetic fields gives

$$\langle \dot{Q} \rangle = 6.9 \times 10^{52} \left(\frac{B}{5 \times 10^{15} \text{G}} \right)^2 \left(\frac{M_\odot}{7M_\odot} \right)^2 \text{ erg s}^{-1} \quad (5)$$

with

$$\left(\frac{B}{5 \times 10^{15} \text{G}} \right) \left(\frac{M}{7M_\odot} \right) = 1.05 \sqrt{\frac{M}{7M_\odot} \frac{20 \text{ s}}{T_{90}}}, \quad (6)$$

where T_{90} refers to the observed durations of long GRBs in seconds.

For the magnetic field strengths in (4) and (6), the mass surrounding the black hole can be estimated on the basis of the stability bound for poloidally magnetized disks by van Putten & Levinson (2003):

$$\frac{\mathcal{E}_B}{\mathcal{E}_k} \simeq \frac{1}{15} \quad (7)$$

following two closely related models for the poloidal magnetic field of energy $\mathcal{E}_B \simeq \frac{1}{6} B^2 R^3$ supported by an inner disk of radius R_D , mass M_D and kinetic energy \mathcal{E}_k . To leading order, we have $\mathcal{E}_k = \frac{GM_M D}{2R_D}$, so that for supermassive and stellar mass black holes

$$M_D \simeq 120 M_\odot \left(\frac{\mathcal{E}_k}{15 \mathcal{E}_B} \right) \left(\frac{R_D}{6 R_g} \right)^4 \left(\frac{M_9^2}{T_7} \right), \quad (8)$$

$$M_D \simeq 0.1 M_\odot \left(\frac{\mathcal{E}_k}{15 \mathcal{E}_B} \right) \left(\frac{R_D}{6 R_g} \right)^4 \left(\frac{M}{7 M_\odot} \right)^2 \left(\frac{20 \text{ s}}{T_{90}} \right) \quad (9)$$

with characteristic matter densities of $7.9 \times 10^{-11} \text{ g cm}^{-3}$ and, respectively, $1.9 \times 10^{11} \text{ g cm}^{-3}$ (close to the neutron drip line). The associated Alfvén velocities $v_A/c = B/\sqrt{4\pi\rho c^2 + B^2}$, where c denotes the velocity of light, are universal, $v_A[\text{AGN}] = 0.1052c$ and, respectively, $v_A[\text{GRB}] = 0.1072c$, and are mildly relativistic.

3. GRBs from rotating black holes

Long GRBs represent the complete life-cycle of a relativistic inner engine (e.g. (Piran & Sari 1998)). The recent *Swift* discovery of the long GRB 060614 poses the challenge to identify a common inner engine to long GBRs with and without supernovae.

In suspended accretion, the evolution of a rapidly spinning black hole ensues on a viscous timescale by spin-down against surrounding high-density matter (van Putten 1999; van Putten & Ostriker 2001). The durations of long GRBs are consistent with the lifetime of rapid spin of a black hole in interaction with high-density matter at its magnetic stability limit (van Putten & Levinson 2003). This applies to newly born, as in core-collapse of a massive stars (Woosley 1993), or in the binary merger of a neutron star with a companion black hole or neutron star. Both scenarios produce a black hole-torus system (van Putten & Levinson 2003).

We searched for the presence of a viscous time-scale in the GRB light-curves of long events in the BATSE catalogue using matched filtering. To this end, we average normalized light curves in durations and count rates, following translations in time, for a best-fit against a template produced by viscous spin-down (Eqs.(7) in van Putten (2008a)). Fig. 1 shows a comparison of the template with the normalized light curves of two notable low-variable, low-luminosity events (Reichert et al. 2001). Because these single Fast Rise Exponential Decay (FRED)-like light events are rare, we next focus on typical, highly variable light curves from a list of consecutive BATSE triggers, and hence with no selection criteria. Fig. 2 shows some typical fits to the template.

Light curves of GRBs are remarkably diverse, and few look similar. Variability in GRB light curves of long events shows a most variable event GRB 990510, and least variable events such as GRB 970508 and GRB 980425, while variability and luminosity are correlated (Reichert et al. 2001). The shortest time-scales of variability reflects intermittency of a long lived inner engine (Piran & Sari 1998). For GRB-afterglow emissions produced by baryon-poor jets (Shemi & Piran 1990; Frail et al. 2001), variability at intermediate and small time scales is expected from unsteady radiation processes and modulations by orientation effects, especially for rotationally powered inner engines. An accretion disk or torus is in a state of forced turbulence (van Putten 1999) and may be precessing (Portegies Zwart & McMillian 2000), and their interactions with the central black hole should be intermittent, but much less so due to time-variability in accretion in the suspended accretion state. Furthermore, the light curves are inherently scaled in energy, photon count rates and durations by their redshifts.

We extract an ensemble average in the form of a normalized light curve (nLC), wherein all short timescale fluctuations have been filtered out relative to the T_{90} of each individual burst by averaging of the individually normalized light curves against a fixed template. In our procedure, we translate and scale the data to fit a template for producing stable zeroing of the bursts by translation in time followed by normalization to permit taking an ensemble average. It filters out variabilities in the ensemble of light curves at sub-dominant time-scales,

and is not focused on studying individual light curves.

Our focus is complementary to the mean spectral properties of GRBs (Fishman et al. 1989), statistics of sub-bursts (Reichert et al. 2001; Quillan et al. 2002), linear temporal profiles in light curves (McBreen et al. 2002) or modeling selected light curves to bright events (Portegies Zwart & McMillian 2000; Lei et al. 2007). Matched filtering is different from earlier approaches based on the BATSE timing signals of the starting time, T_{50} , T_{90} and peak count rates (Mitrofanov et al. 1996; Fenimore 1997). Quite generally, template matching gives stability for burst-alignments and scaling, much more so than BATSE timing signals. On this basis, our results disprove the earlier suggestion of a linear decay in the average GRB light curves (Fenimore 1997), which is also not seen in Mitrofanov et al. (1996).

We have verified that our nLC is stable against a choice of template. Fig. 3 shows very similar results obtained for the Kerr template and block-type template (Fig. 3). The matching procedure is consistent, in that block- and Kerr-type templates produce a match of their FWHM, shown in the lower window of Fig. 3. Matched filtering thus creates an nLC as a unique diagnostic for the underlying slow-time behavior, by filtering out the diversity in GRB light curves due to intermittencies, orientation effects and redshifts.

The exponential decay in the nLC (Fig. 4) is in good agreement with viscous spin-down of Kerr black holes by dissipation of spin-energy in the event horizon which, to leading order, represents a *doubling* the Bekenstein-Hawking entropy

$$S_{H,i} = 2\pi M^2 \rightarrow S_{H,f} = 4\pi M^2, \quad (10)$$

where λ changes from $\lambda_i = \pi/2$ to $\lambda_f = 0$. To next order, the energetic output of the black hole is in various radiation channels by surrounding matter and, to much higher order, in radiation along the spin-axis of the black hole.

The GRB-afterglow arise by dissipation of the kinetic energy in ultra-relativistic baryon-poor jets in internal and external shocks (Shemi & Piran 1990). Modeling by Poynting flux along an open magnetic flux-tube in the force-free limit (Goldreich & Julian 1969; Blandford & Znajek 1977; Thorne et al. 1986) supported by an equilibrium magnetic moment of the black hole surrounded by a uniformly magnetized disk or torus predicts a correlation between the peak energy E_p , the true energy in gamma-rays E_γ and the durations T_{90} as measured in the local rest-frame, given by (van Putten 2008b)

$$E_p T_{90}^{1/2} \propto E_\gamma, \quad (11)$$

showing a Pearson coefficient of 0.85 in the HETE-II and Swift data (Amati et al. 2002; Ghirlanda et al. 2004; Ghisellini et al. 2007), compiled in Fig. 1 of (van Putten 2008b).

We attribute the correlation between variability and luminosity (Reichert et al. 2001) to the angular distribution of beamed outflows from open flux-tubes with a finite horizon opening angle, consistent with observations (Frail et al. 2001). Their output (luminosity density per steradian) increases with angle between the the line-of-sight and the spin-axis of the black hole, reaching its maximum along magnetic field lines suspended at a half-opening $\theta_H \sim M/R_T$ on the event horizon set by poloidal curvature in the inner torus magnetosphere, where R_T denotes the radius of the torus (van Putten & Levinson 2003). The relatively small fraction of spin-energy thus released in true energy in gamma-rays E_γ is in good agreement with the observed estimate of $\sim 10^{51}$ erg (Frail et al. 2001). Conceivably, intrinsic variability in gamma-ray emissions reaches a maximum in the boundary layer with the surrounding baryon-rich torus winds. If so, the *observed* variability and luminosity depend on viewing angle. In the nLC, this orientation effect is effectively averaged out.

4. UHECRs from supermassive rotating black holes

The funnel within an ion torus creates a natural environment for an open magnetic flux-tube along the spin-axis of the black hole, supported by an equilibrium magnetic moment of the black hole when exposed to a surrounding magnetic fields (van Putten 1999). The magnetic field may be intermittent in strength and sign, provided it carries a net poloidal magnetic flux.

A relativistic capillary effect induced by differential frame-dragging acting on open magnetic flux-tubes introduces a linear accelerator upstream of an outgoing Alfvén front illustrated in Fig. 5. Exposure to UV-radiation from an ion torus in AGN Ford et al. (1995) allows for acceleration of ionic contaminants to UHECR energies correlated with the physical properties of the central black hole. Based on (2) and (4, we have

$$\mathcal{E} = 5.6 \times 10^{19} \sqrt{\frac{M_9}{T_7}} \left(\frac{\theta_H}{0.5} \right)^2 \text{ eV}, \quad (12)$$

where an horizon half-opening angle $\theta_H \simeq 30^\circ$ is used as a fiducial value based on M87 (Junor et al. (1999); M87, however, is an FR I source). The underlying magnetic field-energy – which is currently not accessible to direct observations – is here replaced by its correlation to the lifetime of black hole spin, and its identification with the lifetime of FR II radio-galaxies. The correlation (12) is in good agreement with the GZK threshold energy of 6×10^{19} eV for observing UHECRs from nearby AGN.

UHECRs may be powerful probes of spin of supermassive black holes. In our model, the UHECRs are emitted anisotropically preferentially along an finite angle relative to the

spin-axis of the black hole, as in gamma-ray emissions from stellar mass black holes discussed in the previous section. This angle may be appreciable, perhaps as large as 30° on the basis of the opening angle in M87. This picture is consistent with the absence of an UHECR association to BL Lac objects (Harari 2007), which are believed to include both FR I and II sources viewed close to the line of sight – too close perhaps for producing UHECRs.

The maximum luminosity L_j of the baryon-poor jet along an open magnetic flux-tube can be estimated in terms of the fraction $\sim \frac{3}{8} \sin^4 \theta_H$ of $\langle \dot{Q} \rangle$,

$$L_j = L_- + L_+ \simeq 1.3 \times 10^{46} \left(\frac{M_9}{T_7} \right) \left(\frac{\theta_H}{0.5} \right)^4 \text{ erg s}^{-1}, \quad (13)$$

where L_- may drive dissipation in shocks downstream and L_+ may generate ultra-high energy emissions upstream. Here, L_+ depends on the efficiency of mediating the Faraday induced horizon potential to the outgoing Alfvén front: it reaches 100% in the force-free limit envisioned by Blandford & Znajek (1977) when $L_- \simeq 0$. The luminosity in UHECRs depends on the density of ionic contaminants upstream, and their exposure to UV radiation. The observed time-averaged AGN luminosity, considered in Waxman (2004), is here governed by the time-average $\langle \theta_H^4(t) \rangle$, which does not provide a sharp constraint on peak energies in UHECRs. Geometrical considerations suggest $\langle \theta_H^4(t) \rangle \simeq M^4 \langle R_D^{-4}(t) \rangle$ is set by the poloidal curvature in magnetic field lines associated with a time-variable $R_D(t)$, as in the Seyfert galaxy MCG 60-30-15 (Tanaka et al. 1995; Iwasawa et al. 1996). Including the duty cycle, $\langle L_j(t) \rangle$ can hereby be smaller than the peak values (13) by one to two orders of magnitude. Low-luminosity AGN hereby favor UHECR production by allowing for relatively clean sites for particle acceleration. In light of (13), it would therefore be of interest to pursue an observational study of the true ages of Seyfert galaxies. See further (van Putten & Wilson 1999; Farrar & Gruzinov 2008) for related considerations on intermittencies.

In general, therefore, (13) is an upper limit to a luminosity in UHECRs which may be intermittent on time-scales of the light-crossing time of the ion torus – tens of years or less – and extending for the lifetime of spin of the black hole, i.e.: 1-10 M yr, on the basis of observational lifetimes of FR II radio galaxies.

The same principles apply to UHECRs from spinning stellar mass black holes in GRBs. Expressed in total energy output, the relative contributions to the PAO observations satisfies

$$\frac{\mathcal{E}[\text{GRB}]}{\mathcal{E}[\text{AGN}]} \simeq 1.4 \times 10^{-4} \left(\frac{N[\text{AGN}, < 100 \text{ Mpc}]}{500} \right)^{-1}, \quad (14)$$

given 1 long GRB yr^{-1} within 100 Mpc and scaled against a fiducial number of 500 AGN powered by black hole spin within this distance. GRBs appear to be sub-dominant.

5. Conclusions and Outlook

The findings in this paper are part of a study on durations, light curves, spectral properties and correlations to the mass and lifetime of black hole spin:

1. We identify the bi-modal distribution of durations in the BATSE catalogue with hyper- and suspended accretion on slowly and rapidly spinning BHs (Eqs.(7-8) and Eqn.(9), respectively, in van Putten & Ostriker (2001)). The time scale of hyperaccretion onto slowly spinning black holes is $\sim t_{ff}\mathcal{E}_k/\mathcal{E}_B \simeq$ tenth's of seconds, where t_{ff} denotes the free fall timescale. Black hole angular velocities that are slower and faster than the angular velocity at the ISCO thus give rise to transient sources to the left and, respectively, to the right of the break at ~ 2 s separating the two classes in the BATSE catalogue. Unification on the basis of black hole spin rates predicts low-luminosity X-ray afterglows also to short GRBs (van Putten & Ostriker 2001), confirmed by *Swift* in GRB 050709 and HETE II in GRB 050509B. This unification does not require (but does not rule out) different values of the magnetic field strength and the mass of the black hole.
2. We report on an exponential decay in the BATSE catalogue of light curves of long GRBs in agreement with viscous spin-down of a Kerr black hole. The quality of the fit to the model template by matched filtering shows that long GRBs are to leading order a process of doubling the entropy of the event horizon, expressed in (10).
3. We describe a common inner engine to unify long events GRB 030329/SN2003h and GRB 060614 with and without supernovae, produced in CC-SNe (Woosley 1993; Paczynski 1998) and the binary merger of a neutron star with a rapidly spinning black hole (van Putten 1999) or a companion neutron star (Fig. 1 in van Putten & Levinson (2003)).
4. Our model predicts a spectral-energy correlation (11) in agreement with HETE II and *Swift* data with a Pearson coefficient of 0.85 (Fig. 1 in van Putten (2008b)).
5. Our model predicts UHECRs with energies (12) correlated to the mass of the central black hole and the lifetimes of AGN in agreement with PAO data, and emitted anisotropically consistent with the paucity of UHECRs from BL Lac objects.

For GRBs, accretion-powered models (e.g (Woosley 1993; Kumar et al. 2008) are different. They do not account for GRB060614, since it was not a core-collapse event (Della Valle 2006). Winds from the inner disk, at typical temperatures of 1-2 MeV, are too contaminated to produce the ultra-relativistic (baryon-poor) outflows needed to account for the observed

GRB-afterglow emissions and spectral-energy correlations. If attributed to the central black hole, then its spin *up* by continuing accretion (Kumar et al. 2008) is at odds with the decay in BATSE data (Fig. 1).

Late-time X-ray emissions on a timescale of 1-10 k s – distinct from X-ray afterglows to the prompt GRB-emissions – are observed by *Swift* in a number of long GRBs (see Zhang (2007) for a review). They can be attributed to late-time infall of the outer envelope of a remnant progenitor star in core-collapse events (Kumar et al. 2008). Late-time infall onto a black hole, regardless of spin, may be expected to be luminous as matter forms high-densities in the process of free fall (as in SN1987A). In the absence of a massive progenitor star, as in mergers of a neutron star and a black hole or mergers of two neutron stars, we anticipate that events such as GRB 060614 – and more generally long GRBs with anomalously low-luminosity X-ray afterglow emissions, identified with binary mergers in low density environments – feature no or relatively weak late-time X-ray emissions. Weak late-time X-ray emissions is expected, since the break-up of the neutron star(s) in a binary merger is known to be potentially messy, leaving matter at relatively large radii to fall in with appreciable time delay. This may be verified observationally, by searching for late-time X-ray emissions in long GRBs without supernovae and GRBs – long and short – with anomalously low X-ray afterglows to their prompt GRB emissions.

To illustrate our unification scheme, we interpret some pivotal GRBs as follows:

GRB 050709, GRB 050509B (*short GRBs with X-ray afterglows*). Binary mergers of a neutron star with a slowly spinning black hole, producing a short duration event in a state of hyperaccretion. The GRB-afterglows were produced by black hole outflows, interacting with a low-density environment.

GRB 030329 (*long GRB-supernova*). Core-collapse of a massive star, producing a long duration event in a state of suspended accretion. GRB-afterglow emissions were produced by black hole outflows from a rapidly spinning black hole, interacting with high-density environments typical for star-forming regions.

GRB 050911 (*long GRB without X-ray afterglow*). The binary coalescence of a neutron star with a rapidly spinning black hole or the merger of two neutron stars, giving rise to a long duration event in a state of suspended accretion. The absence of an X-ray afterglow is attributed to the low-density environment typical for binaries.

GRB 060614 (*long GRB without supernova*). Binary coalescence of a neutron star with a rapidly spinning black hole or the merger of two neutron stars, given rise to a long duration event in suspended accretion without a supernova. The relatively low-luminosity X-ray plateau is attributed to a limited amount of late-time infall of remnant matter following the break-up of the neutron star(s).

GRB 070110 (*long GRB with late-time X-ray emissions*). A core-collapse of a massive star

GRB-supernova with late-time X-ray emissions from fall-back of matter from the remnant stellar envelope (Kumar et al. 2008).

GRB 080319B (*luminous and variable long GRB*). A GRB viewed along the boundary of a baryon-poor jet, where the luminosity and variability is highest subject to instabilities in interaction with surrounding baryon-rich disk winds.

If GRBs and the recently reported short duration radio burst (if confirmed) are related, then long-duration radio-bursts may exist associated with events like GRB 060614 or, more generally, with long duration bursts with anomalously weak X-ray afterglows.

Complete optical-radio surveys of the local transient universe promise to provide a valuable catalogue of core-collapse supernovae, radio-loud SNe and radio-bursts. These surveys can be optimized by scanning along the local super-clusters, avoiding the large-area voids in between (Einasto et al. 1994). They may be augmented by large neutrino detectors (Shin’ichiro et al. 2005) to provide real-time triggers of the onset of supernovae as in SN1987A. The Australian MOST survey illustrates surveys of radio-loud SNe, all of which are CC-SNe, few of which will be associated with long GRBs in view of a branching ratio of a mere 0.2-0.4% of Type Ib/c into GRBs (van Putten 2004). Augmented by optical surveys, e.g., by Pan-STARRs (in the northern hemisphere), these surveys could provide targets of interest to LIGO and Virgo, to study a possibly common inner engine to Type II and Type Ib/c SNe, perhaps similar to those at work in GRBs, the latter which are expected to have a long duration bursts in gravitational waves with negative chirp. The CC-SNe scenario for long GRB-SNe requires a companion star in close binary orbit to ensure rapid rotation by tidal interaction (Paczynski 1998). At present, a companion has only been identified to the Type II/Ib SN 1993J event (Maund et al. 2004), otherwise not known to have been a GRB.

The FR I and II classification expresses a dichotomy in radio-galaxies Fanaroff & Riley (1974), as in 3C31 and Pic A. The FR II sources are lobe-dominated and edge-brightened, straight and one-sided (on the kpc scale), which is testimony to their power, exceptional long-term orientation stability and radiation beaming in relativistic outflows. It suggests that FR IIs may be associated with black hole spin, more likely so than the probably accretion powered FR Is (Baum et al. 1995). But, the FR II’s may not be the only AGN harboring rapidly spinning black holes. Follow-up PAO statistics on UHECRs will be important in confirming the association with AGN, and in identifying the type of AGN, host galaxies and their orientation relative to the line-of-sight. We suggest that spinning black holes may be hosted in Seyferts and LINERs, producing largely leptonic outflows and emissions in UHECRs without baryon-rich disk winds. UHECR-active AGN without FR II morphology may be understood by the absence of disk winds, perhaps due to weak poloidal magnetic fields. When radio-jets do form, polarization studies on FR I and II jets show large-scale ordered magnetic fields with

more pronounced toroidal magnetic fields in FR II sources. Black hole spin interacts largely with the inner disk, through the *time-average* of energy-density of net poloidal magnetic flux, while UHECR production is associated with *instantaneous* poloidal magnetic flux along an open flux-tube with finite opening angle set by a generally time-variable radius of the inner disk. The outflows will remain largely baryon-free in the absence of outer disk winds (cf. the X-ray jet of the Crab pulsar (Lu et al. 2001)), inhibiting dissipation in shocks to re-accelerate charged particles (cf. modeling GRB-afterglows (Shemi & Piran 1990)). There may therefore be anomalously weak or unseen extended radio-emissions associated with intermittent UHECR production from clean sites for acceleration in Seyfert galaxies, where the details may be constrained by the lifetime of Seyfert galaxies.

Acknowledgment. We thank the referee for a number of thoughtful comments and Ski Antonucci, Gilles Theureau and Ismaël Cognard for stimulating discussions. This work is supported, in part, by a grant from the Région Centre of France.

REFERENCES

- Abraham, J., et al., (Pierre Auger Collaboration), 2007, *Science* 318, 938
- Amati, L., Frontera, F., Tavani, M., et al., 2002, *A&A*, 390, 81A; Nava, L., Ghisellini, G., Ghirlanda, G., et al., 2006, *A&A*, 450, 471; Campana, S., Guidorzi, C., Tagliaferri, G., et al., 2007, *A&A*, 472, 395
- Antonucci, R., 1993, *ARA&A*, 31, 473
- Antonucci, R., 2008, priv. comm.
- <http://brussels2008.aspera-eu.org>
- Baum, S. A., Zirbel, E. L., & O’Dea, C. P. 1995, *ApJ*, 451
- Bekenstein, Jacob D., 1973, *PRD* 7, 2333; Bardeen, J. M., Carter, B., Hawking, S. W., 1973. *Commun. Math. Phys.* 31, 161; Hawking, Stephen W., 1974, *Nature*, 248; A. Strominger, C. Vafa, 1996, *Phys. Lett. B* 379,99
- Blandford, R.D., & Znajek, R.L., 1977, *MNRAS*, 179, 433
- Della Valle, M., et al., 2006, *Nature*, 444, 1050; Fynbo, J.P.U., et al., 2006, *Nature*, 444, 1047; Gerhels, N., et al., *Nature*, 444, 1044; Gal-Yam, A., et al., 2006, *Nature*, 444, 1053; Amati, L., Della Valle, M., Frontera, F., et al., *A&A*, 2007, 463, 913

- Eichler, D., & Jontof-Hutter, D., 2005, *ApJ*, 635, 1182
- Einasto, M., et al., 1994, *MNRAS*, 269, 301
- Fanaroff, B.L., & Riley, J.M., 1974, *MNRAS*, 167, 31P
- Fenimore, E.E., 1997, *astro-ph/971233*
- Farrar, G.R., & Gruzinov, A., 2008, *astro-ph/0802.1074*
- Ford, L.A., et al., 1995, *ApJ*, 439, 307
- Frail et al., 2001, *ApJ*, 562, L55
- Fraschetti, F., 2008, *astro-ph/0809.3057*
- Fraschetti, F., & Melia, F., 2008, *astro-ph/0809.3686*
- Fishman, G.J., et al., 1989a, in *Proc. GRO Science Workshop, Vol. 2*, ed. N. Johnson (Washington, DC: NRL), 39; Fishman, G.J., et al., in *Proc. GRO Science Workshop, Vol. 3*, ed. N. Johnson (Washington, DC: NRL), 47; Pendleton, et al., 1994, *ApJ*, 431, 416; Kaneko, Y., et al., 2006, *ApJ. Suppl.*, 166, 298
- Ghirlanda, G., Ghisellini, G., & Lazzati, D., 2004, *ApJ*, 616, 331;
- Ghisellini, G., Celotti, A., Ghirlanda, G., Firmani, C., & Nava, L., 2007, *MNRAS*, 382, L72
- Ghisellini, G., et al., 2008, *MNRAS*, 390, L88
- Goldreich, P., & Julian, W.H., 1969, *ApJ*, 157, 869
- Harari, D., 2007, 30th International Cosmic Ray Conference, Merida, Mexico, July 2007; *astro-ph/0706.1715*
- Iwasawa, K., Fabian, A.C., & Reynolds, C.S., et al., 1996, *MNRAS*, 282, 1038
- Jackson, C., & Wall, J.V., 1999, *MNRAS*, 304, 160
- Junor, W., Biretta, J.A., Livio, M., 1999. *Nature* 401, 891
- Kerr, R.P., 1963, *Phys. Rev. Lett.*, 11, 237
- Kumar, P., Narayan, R., Johnson, J.L., 2008, *Science*, 321, 376; *ibid.* 2008, *MNRAS*, 388, 1729
- Lei, W.H., Wang, D.X., Gong, B.P., & Huang, C.Y., 2007, *A&A*, 468, 563

- Levinson, A., *in* High Energy Gamma-Ray Astronomy, 2000, Heidelberg, Germany. AIP Proc., 558. Edited by Felix A. Aharonian and Heinz J. Vlk. (AIP, Melville, New York), p.798
- Livio, M., Ogilvie, G. I., & Pringle, J. E. 1999, ApJ, 512
- Lorimer, D.R., et al., 2007, Science, 318, 777
- Lu, F.J., Aschenbach, B., Song, L.M., & Durouchoux, Ph., 2001, ApSSS, 276, 141L
- Maud, J.R., et al., 2004, Nature, 427, 129
- McBreen, S., McBreen, B., Hanlon, L., & Quillan, F., 2002, A&A, 293, L15; McBreen, S., McBreen, B., Hanlon, L., & Quillan, F., 2002, A&A, 293, L29
- Mitrofanov, I.G., et al., 1996, ApJ, 459, 570
- Mioduszewski et al., 2004, NRAO/AUI/NSF (<http://www.nrao.edu/pr/2004/ss433/>)
- Moskalenko, I.V., et al., 2008, astro-ph/0805.1260
- Nagar, M., & Matulich, J., 2008, A&A, 488, 879
- O’Dea, C.P., et al., 2008, A&A, to appear
- O’Sullivan, S.P., & Gabuzda, D.C., 2008, in Proc. 9th EU VLBI Network Symposium: The role of VLBI in the Golden Age for Radio Astronomy and EVN Users Meeting, Bologna, Italy
- Paczynski, B.P., 1998, ApJ, 494, L45.
- Papapetrou, A., 1951, Proc. Roy. Soc., 209, 248; *ibid.* 259
- Piran, T., & Sari, R., 1998, in 18th Texas Symp. Relat. Astroph. Cosmology, A.V. Olinto, J.A. Friedman, D.N. Schramm, Eds. (World Scientific, Singapore), pp. 34
- Portegies Zwart S.F. and McMillain S.F.W., 2000, ApJ, 528, L17
- Quilligan, F., McBreen, B., & Hanlon, L., et al., 2002, A&A, 385, 377
- Reichert, D.E., Lamb, D.Q., & Fenimore, E.E., et al., 2001, ApJ, 552, 57; Reichert, D.E., & Lamb, D.Q., 2001, in Procs. of Gamma-Ray Bursts in the Afterglow Era, ed. E. Costa, F. Frontera, & J. Hjorth (Springer Verlag)

- Shemi, A., & Piran, T., 1990, ApJ, 365, L55; Rees, M.J., & Mészáros, P., 1992, MNRAS, 258, 41; Rees, M.J., & Mészáros, P., 1993, ApJ, 418, L59; Rees, M.J., & Mészáros, P., 1994, ApJ, 430, L93; Mészáros, P., & Rees, M.J., 1997, MNRAS, ApJ, 476, 232; Wijers, R.A.M.J., Rees, M.J., & Mészáros, P., 1997, MNRAS, 288, L51; Reichart, D.E., 1997, ApJ, 485, L57; Piran, T., 1998, Phys. Rep., 314, 575; Piran, T., 1999, Phys. Rep., 314, 575; Piran, T., 2000, Phys. Rep., 333, 529; Garcia, M.R., Callanan, P.J., & Moraru, D., et al., 1998, ApJ, 500, L105; Mészáros, P., 2002, ARA & A, 40, 137
- Shin'ichiro, A., Beacom, J.F., & Hasan, Y., 2005, Phys. Rev. Lett., 95, 171101
- Tanaka, Y., Nandra, K., & Fabian, A.C., 1995, Nature, 375, 659
- Thorne, K.S., Price, R.H., & McDonald, D.H., 1986, *Black Holes: The Membrane Paradigm* (Yale University Press, New Haven, CT)
- Urry, C.M., & Padovani, P., PASP, 107, 803
- van Putten, M.H.P.M., & Wilson, A., http://online.kitp.ucsb.edu/online/bhole_c99/
- van Putten, M.H.P.M., 1999, Science, 284, 115
- van Putten Ostriker, 2001, ApJ 552 L31
- van Putten & Levinson, A., ApJ, 584, 937; van Putten, M.H.P.M., 2003, 583, 374 *ibid.* 2004, ApJ, 611, L81
- van Putten, M.H.P.M., 2008a, ApJ, 684, L91;
- van Putten, M.H.P.M., 2008b, ApJ, 685, L63
- van Putten, M.H.P.M., 2000, Phys. Rev. Lett., 84, 3752
- van Putten, M.H.P.M., 2004, ApJ, 611, L81
- van Putten, M.H.P.M., 2005, Nuov. Cim. C, 28, 597
- Wald, R.M., Phys. Rev. D., 10, 1680
- Waxman, E., 2004, Pramana, 62, 483; astro-ph/0310079
- Véron-Cetty, M.-P., & Véron, P. 2006, A&A, 455, 773
- Woosley, S.L., 1993, ApJ, 405, 273; Paczyński, B.P., 1998, ApJ, 494, L45

Zaw, I., Farrar, G.R., & Greene, J.E., 2008, astro-ph/0806.3470

Zhang, B., 2007, Adv. Space Res., 40, 1186

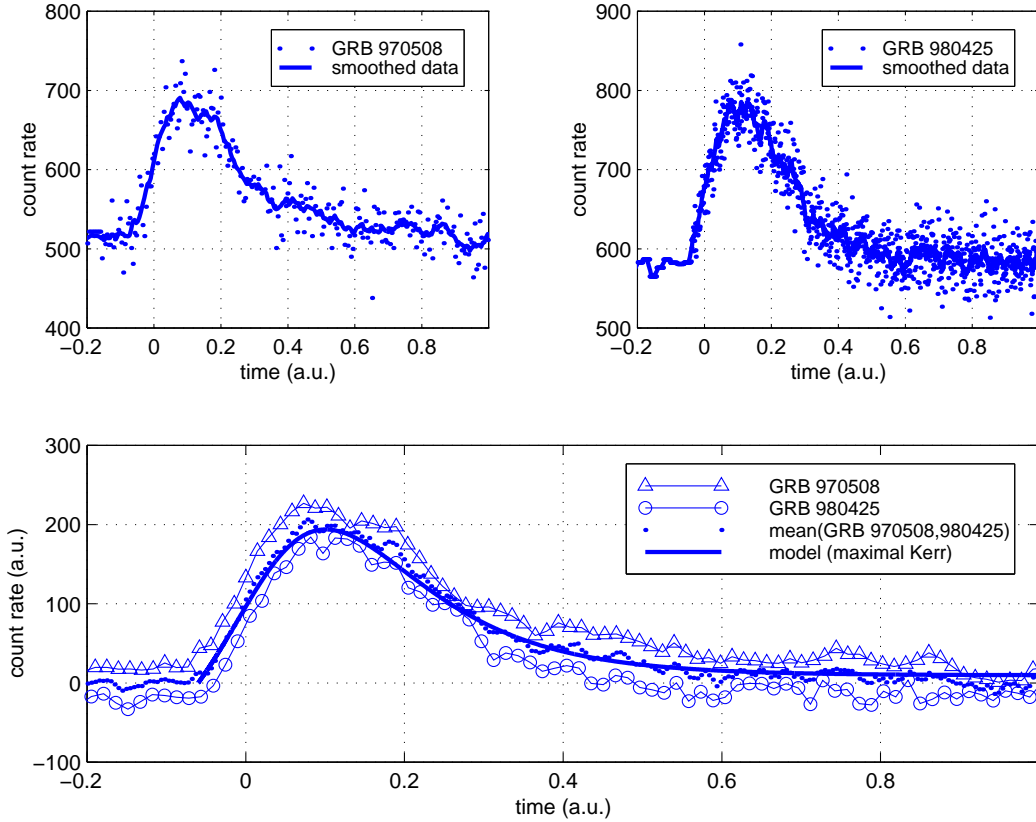


Fig. 1.— A comparison of two low-variability events GRB 970508 and GRB 980425 and a template light curve for GRBs from rotating black holes. The two events display a characteristic fast-rise and exponential decay (FRED). The data are scaled in duration and count rate to compare their shape with the template. Note that the true time-of-onset t'_0 is slightly before the $t_0 = 0$ in BATSE timing.

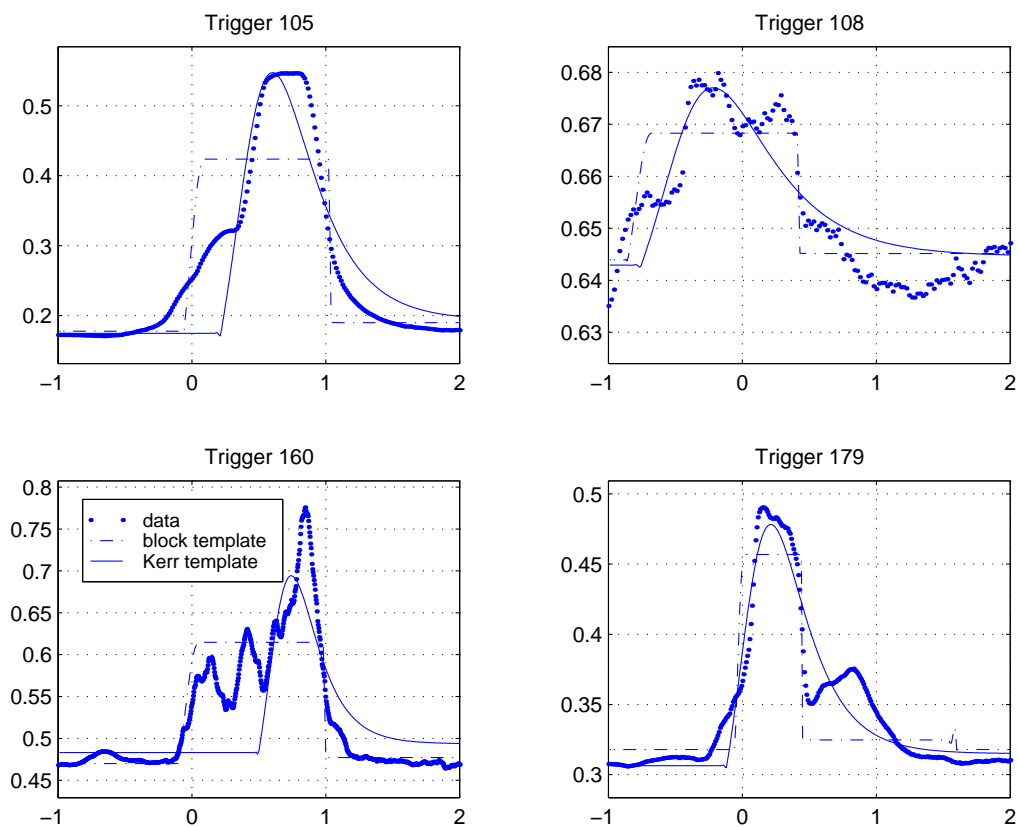


Fig. 2.— Shown are examples of template fits to various long bursts with normalized durations in the sample L1: $2 \text{ s} < T_{90} < 20 \text{ s}$, for both block-type and Kerr template. In each window, the horizontal axis refers to normalized time (a.u.) and the vertical axis refers to normalized count rates (a.u.). Fitting to a template gives a zeroing of the burst by translations in time defined on the basis of the entire shape of the burst relative to the template, illustrated by Trigger 160, different from using special instants such as the BATSE t_0 data. Light curves are subsequently normalized and averaged to produce a normalized light curve.

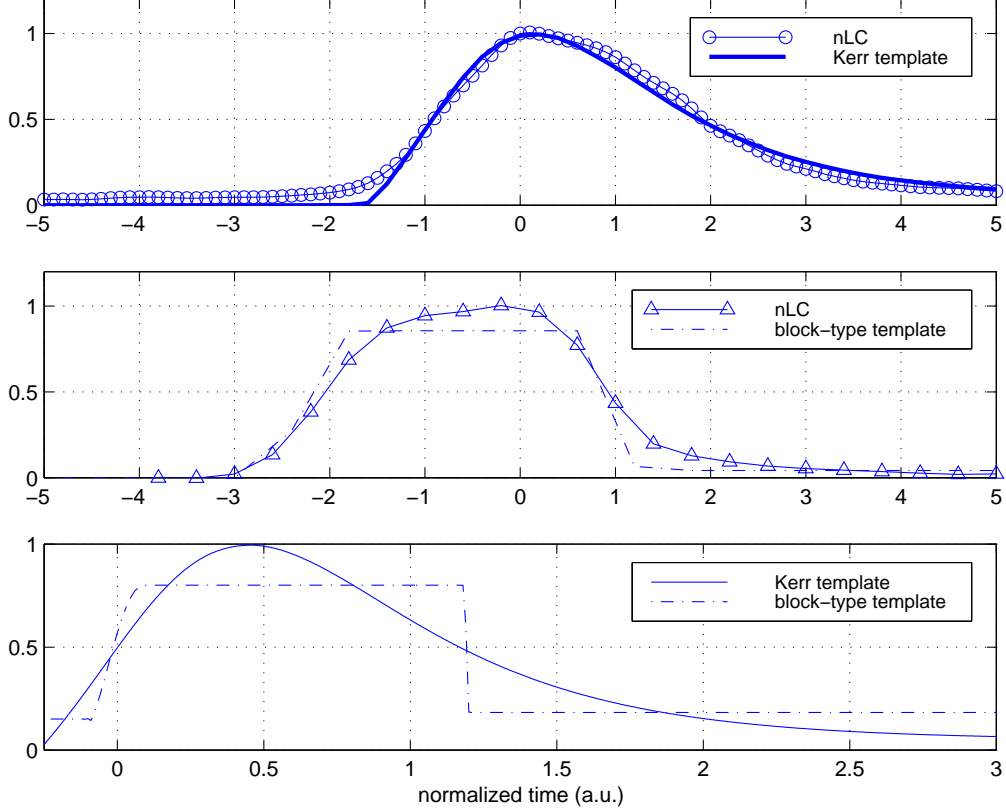


Fig. 3.— Shown are the normalized light curves (nLC) based a Kerr template and a Kerr type template for 300 blindly selected long duration events in sample L1: $2 \text{ s} < T_{90} < 20 \text{ s}$. In each window, the vertical axis refers to normalized count rates (a.u.). The true nLC has the unique property that it matches its template, which applies to the Kerr (*top*) but not the block-type template (*middle*). Note a slightly smoothed average of the block-type templates, due to numerical imperfections in template overlapping. Matching respects the FWHM of the two templates (*bottom*).

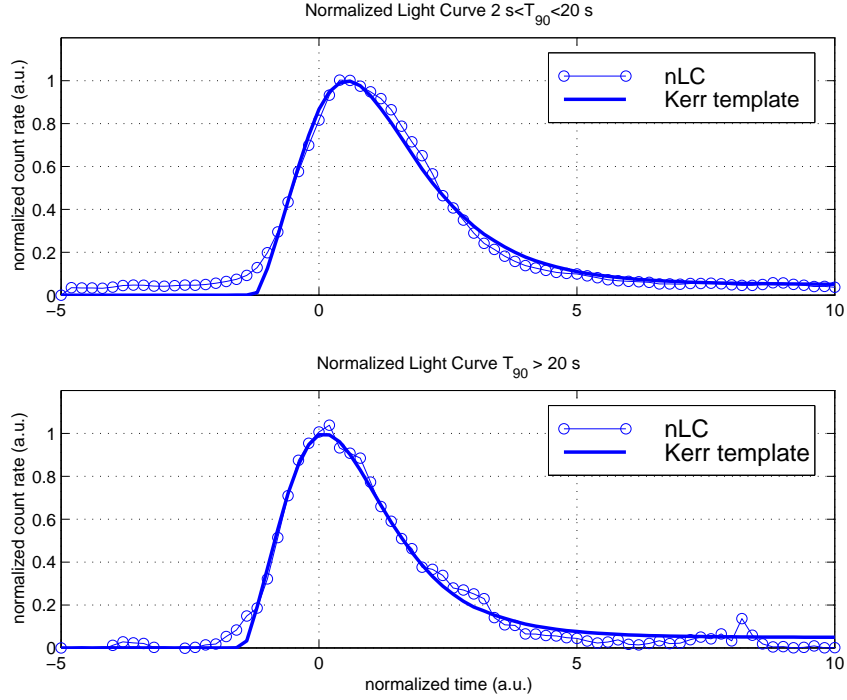


Fig. 4.— The ensemble average of light curves of long GRBs in the BATSE catalogue is the normalized light curve (nLC), obtained by averaging 300 normalized curves of blindly selected long events in sample L1: $2 \text{ s} < T_{90} < 20 \text{ s}$ (*top*) and 300 blindly selected long events in L2: $T_{90} > 20 \text{ s}$ (*below*). The normalizations are based on matched filtering, here against the theoretical template representing viscous spin-down of a Kerr black hole. Convergence of the nLC is slower in L2 than in L1, which may be attributed to frequent intermediate periods of quiescence or dead-periods in the actual GRB light curves. The results show excellent agreement between the theory of viscous spin-down, corresponding to a nearly doubling of the Bekenstein-Hawking entropy of the event horizon.

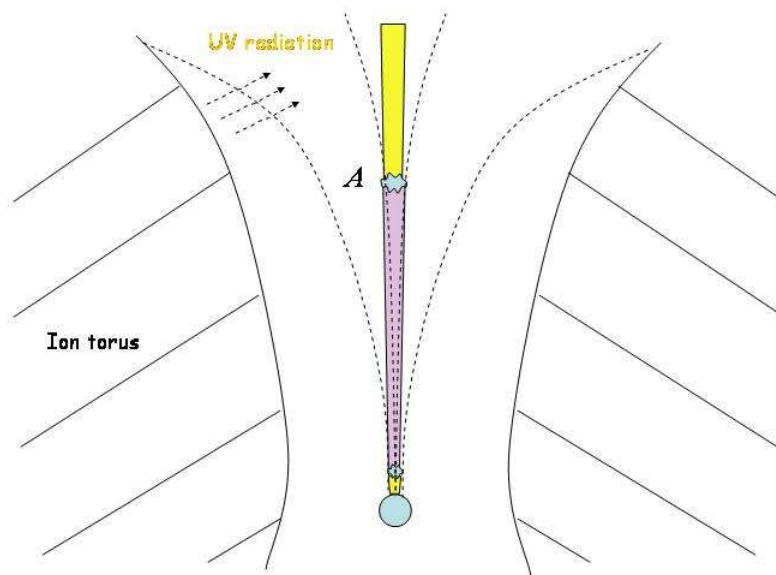


Fig. 5.— The coupling of the Riemann tensor and angular momentum of charged particles creates a relativistic capillary effect, whereby pairs are extracted from the vicinity of the black hole to large distances. The outflow becomes largely force-free up to an outgoing Alfvén front A , which mediates a Faraday-induced horizon Fermi-level to large distances along equipotential magnetic flux-surfaces. Upstream of A , the magnetic flux-surfaces are essentially charge free, and stable against pair-cascade at large distances from the black hole. (Here, frame-dragging is negligible, as it decays with the cube of the distance from the black hole.) As ions are produced from stray particles by exposure from UV-radiation from an ion torus, as in the 60 light-year diameter torus of M87, they are subject to linear acceleration by the generating voltages at the Alfvén surface (which are increasing with poloidal angle away from the polar axis). The linear accelerator here forms in particular to intermittent sources, on a time-scale less than the crossing time of the radius of the ion torus.